J. Chem. Sci., Vol. 122, No. 2, March 2010, pp. 279–285.

Influence of magnetic field on the electrodeposition of Ni–Co alloy

MEHDI EBADI*, W J BASIRUN and YATIMAH ALIAS

Department of Chemistry, Faculty of Science, University of Malaya, 50603 Kuala Lumpur, Malaysia
e-mail: Mehdi_2222002@yahoo.com

MS received 1 June 2009; revised 9 October 2009; accepted 26 October 2009

Abstract. The electrodeposition of Ni–Co alloy from a nickel Watt's solution in the absence and presence of a permanent parallel magnetic field (PPMF) to the plane of deposition (perpendicular to direction of current) produced a deposited layer with mostly fine grain structure. The deposited layers have been characterized by scanning electron microscopy (SEM) and energy dispersive X-ray (EDX). It was found that the mass deposition rate with PPMF was greater than the deposition in the absence of PPMF, where the rate of difference electrodeposited mass (Δm) was calculated (Δm = 0·07 to 0·12 mg $cm^{-2}min^{-1}$). In the presence of PPMF, the electrodeposition of cobalt was high (0 to 5%) compare to the absence of PPMF. The corrosion resistance of Ni–Co alloy layers fabricated by PPMF proved higher than without PPMF.

Keywords. Ni–Co alloy; magnetic electrodeposition; deposition rate.

1. Introduction

Alloy deposition of two or more metals has been carried out to improve properties such as grain size, hardness and corrosion resistance than the parent metals. The deposition of face centered cubic (FCC) Ni–Co alloy coatings has been widely used for recorder head materials in computer hard drives and in surface finishing industries for items such as printed circuit boards, wear resistant coating, corrosion resistance layers, electroformed laser mirrors and decorative coating.[1,2] During alloy deposition, anomalous behaviour can arise when the less noble metal (cobalt) is preferentially deposited compared to the more noble metal (nickel). This phenomenon was described and classified by Brenne.[3] Hessami and Tobias[4] developed a mathematical model for the mass transfer equations where they explained pH influence on the deposition rate. Plieth and Georgiev[5] purposed that the enhanced deposition factor is related to the kink site position. Furthermore, an applied PPMF has a large influence on the mass transport and the deposit morphology.[6–9] In the absence of permanent perpendicular magnetic field (PPMF), the mass transport factors which can control the electrode process are diffusion, ionic migration and convection (natural and forced). With the application of a PPMF, forces such as paramagnetic force ($\vec{F}_P$), field gradient force ($\vec{F}_B$), Lorentz force ($\vec{F}_L$), electrokinetic force ($\vec{F}_E$) and magnetic damping force ($\vec{F}_D$) can become prominent in an electrode reaction, and all forces have units of force per unit volume (N m^{-3}).[10]

Three types of forces which depend on the interaction of the current or movement of ions with the magnetic field are the Lorentz force ($\vec{F}_L$), electrokinetic force ($\vec{F}_E$) and the magnetic damping force ($\vec{F}_D$), while the other two depend on properties of the ions in a magnetic field. The Lorentz force $\vec{F}_L = \vec{j} \times \vec{B}$, is a product of the current density which flows perpendicular to the magnetic field.[9,10] The Electrokinetic force

$$\vec{F}_E = \frac{\sigma_d E_{\Pi}}{\delta_o}$$

is from the effects of the Lorentz force on the charge density in the diffusion layer which gives rise to a non-electrostatic field parallel to the working electrode surface which induces motion of the solution near the interface. σ_d is the charge density in the diffuse layer, $E_{\parallel}$ is the induced non-electrostatic field and δ_o is the diffusion layer thickness. The magnetic damping force results from the damping of the flow of the ions, and $\vec{F}_D = \sigma \vec{v} \times \vec{B} \times \vec{B}$, where $\vec{v} \times \vec{B}$ is the electrostatic field from the interaction between the

*For correspondence

current and the magnetic field, and σ is the solution conductivity.[10]

The Paramagnetic force

$$\vec{F}_P = \frac{\chi_m B^2 \vec{\nabla} c}{2\mu_o}$$

is caused by the difference of paramagnetic susceptibility which arises from the concentration gradient of the paramagnetic ions in the diffusion layer. The field gradient force,

$$\vec{F}_B = \frac{\chi_m c B \vec{\nabla} B}{\mu_o},$$

arises from the non-uniformity of the magnetic field, where B is the magnetic field strength, c is concentration, $\vec{\nabla}B$ is the magnetic field gradient, $\vec{\nabla}c$ is the concentration gradient and μ_o is the permeability of free space.[10]

Thematically, these two forces $\vec{F}_P$ and $\vec{F}_B$ depend on magnetic moment (μ) and molar susceptibility (χ_m) of elements which are related to the number of unpaired valence electrons. The magnetic moments for metal ions has shown by Carlin.[10] The field gradient force $\vec{F}_B$ and Paramagnetic force $\vec{F}_P$ depends on the magnetic susceptibility of the atoms or ions. From elementary theory of magnetochemistry, the magnetic susceptibility can be expressed as, $\chi_m = N\mu_o\mu^2/3kT$, where N is the number of molecules per unit volume, μ is the magnetic moment of the atom or ion, μ_o is the magnetic permeability of vacuum, k is Boltzmann constant and T is absolute temperature.[11] The molar susceptibility (χ_m) for paramagnetic ($\chi_m > 0$) and diamagnetic ($\chi_m < 0$) materials is maximum if the applied PPMF is perpendicular to current density and vice versa.[10] In the present study, the paramagnetic ions such as nickel and cobalt were chosen to the co-deposition of Ni–Co alloys on a diamagnetic substrate such as copper. This paper investigates the electrodeposition of paramagnetic ions (Ni and Co) to produce Ni–Co alloy with an applied PPMF and without a PPMF and investigates the alloy properties from those two conditions of electrodeposition.

2. Experimental

The electrodeposition of Ni–Co alloys in the absence and presence of a PPMF was carried out on copper substrates (0·01 × 1 × 2 cm) using an electrochemical cell with a conventional Nickel Watt's solution given in table 1. The pH was adjusted to 4 ± 0·1 by adding sulphuric acid. Current density was maintained at 75 mA cm^{-2} with temperature between 50 and 55°C. The electrochemical cell made from Teflon (10 × 6 × 3 cm) which was used for electrodeposition of Ni–Co in the presence and absence of PPMF is shown in figure 1. Two copper plates held back to back was at the same distance to the nickel anodes in which one of them faced the magnetic field, and another away from the magnetic field. The distance between the cathode and nickel anode was 4·5 cm. A permanent magnetic field (4·4 T) was placed perpendicular to current flow between the anode and cathode and parallel to the

Table 1. The composition of Nickel Watt's solution mixed with different amounts of Co^{2+} ion (X; 0, 4·5, 13·2, 17·4, 21·6 g l^{-1}) to the electrodeposition of Ni and Ni–Co alloy at the presence and absence of PPMF.

Sample	Component salts	Concentration (g l^{-1})
Ni–Co	$NiSO_4{\cdot}6H_2O$	260
	$NiCl_2{\cdot}6H_2O$	60
	H_3BO_3	40
	Thiourea	0.2
	$CoSO^4{\cdot}7H_2O$; (Co^{+2})	X; 0, 4·5, 13·2, 17·4, 21·6

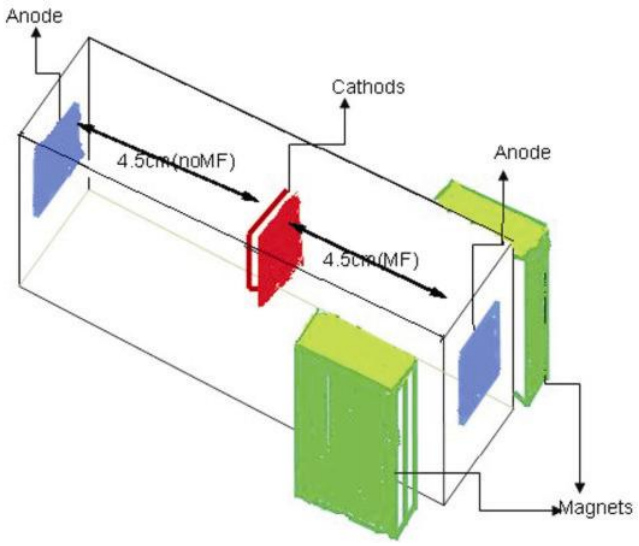

Figure 1. Schematic diagram of the experimental set-up. A Teflon cell (10 × 6 × 3 cm), cathodes plate are two copper (2 × 1 cm) which held by 4·5 cm from Ni anodes. The one copper plat faced to perpendicular MF (4·4T), another one faced to without MF zone.

surface of the cathode. Before electroplating, copper plates were chemically polished by immersion into an acid mixture of HCl, H_2SO_4, CrO_3 and HNO_3 for a few seconds and then rinsed with distilled water. The mass Ni–Co alloy electrodeposited layers were calculated from the difference of mass before and after electrodeposition on the copper plates.

The Ni–Co electrodeposits were analysed using energy dispersive X-ray (EDX) system INCA energy 400). The Ni–Co electrodeposited is analysed from an X-ray diffraction (D^8 – Advanced XRD) set using a CuK_α radiation with wavelength 1·540 Å. Corrosion measurements were done using FRA software Autolab PGSTAT-302N. The seawater of 3·5% salinity was used as the corroding solution in the corrosion process.[12] Platinum wire and saturated calomel electrode (SCE) were chosen as the counter and reference electrodes. The solution was carefully de-aerated from oxygen before corrosion measurement with nitrogen. In electrochemical impedance spectroscopy (EIS) measurements, the frequency range was set between 10 kHz and 0·01 Hz. The surface ratio of counter and working electrodes were set at 1 : 1 in the corrosion process.

3. Results and discussion

3.1 *Mass deposition rate*

Electrodeposition rate is the amount of metal deposited (g) per unit time (t).[3] Electrodeposition rate depends on many factors such as electric potential, electrode parameters (material, surface state, shape, etc.) and electrolyte parameters (composition, concentration, conductivity, pH, etc.).[13] Several investigators have reported that the electrodeposition of cobalt[14–18]and nickel[19–21] are mass transport controlled. Based on this the electrodeposition of nickel–cobalt alloy under magnetic field in this work is also under the influence of mass transport. Convection can enhance the deposition rate through the mechanical agitation of the electrolyte. Convection can also be increased with an applied magnetic field during electrodeposition. The Lorentz force ($\vec{F}_L$), is generated from the interaction of a permanent magnetic field perpendicular to the current flow.[22–24] Figure 2 shows mass deposition rate (g cm^{-2} min^{-1}) vs cobalt concentration (g l^{-1}) in nickel Watt's bath. In figure 2, the difference in mass electrodeposition rate Δm (with and without PPMF), was calculated having a range from 0·07 to 0·12 mg cm^{-2} min^{-1}. Cobalt is one of the elements that have excellent ferromagnetic properties.[10] Using a Co concentration of 8·9 g l^{-1} in the Ni Watt's bath, EDX results gave 45 and 40% Co content in the Ni–Co alloy in the presence and absence of a PPMF, respectively. While Ni^{2+} and Co^{2+} are both double charged ions and thus will experience almost the same Lorentz force which enhance the deposition of Ni and Co to the same extent. Because of the larger magnetic moment of Co compared to Ni, the Field Gradient force F_B and Paramagnetic force F_P will become larger for Co than for Ni, thus increasing the Co content in the electrodeposited Ni–Co alloy in the presence of a PPMF.

Table 2 gives the Electrodeposition efficiency with different contents of cobalt in Nickel Watts bath. The current efficiency for Ni–Co electrodeposition can be calculated from the Faraday's law

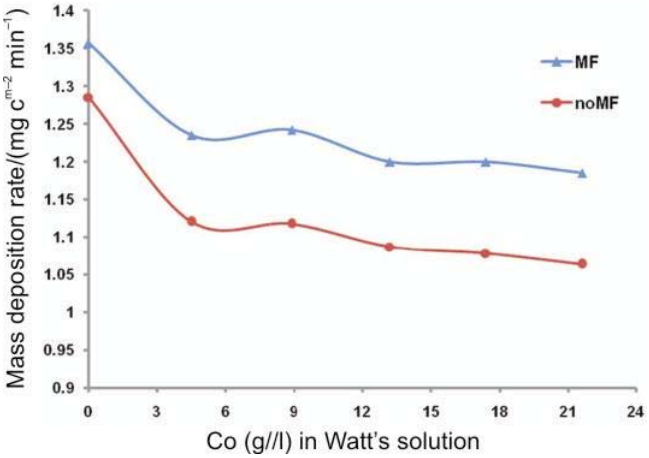

Figure 2. The mass electrodeposition rates of Ni–Co alloy in the presence (4·4 T) and absence of PPMF with different concentration of cobalt in Ni Watt's bath.

Table 2. The % efficiency of electrodeposition was enhanced with PPMF compare to without of PPMF for each solution.

Co(g/l) in Ni Watt's solution	% Efficiency of deposition with PPMF	% Efficiency of deposition without PPMF
0	97·9	93·8
4·5	90·1	81·8
8·9	90·6	81·6
13·2	87·5	79·3
17·4	87·5	78·6
21·6	86·5	77·6

$$\phi = \frac{mnF}{tAjM} = \left(\frac{m}{tA}\right)\left(\frac{nF}{jM}\right),$$

where m = mass of electrodeposition/g, t = electrodeposition time/s, A = surface area of deposition/m^2, n = number of electron involved in reduction of nickel and cobalt ions, F = Faraday constant/C mol^{-1}, j = current density/A m^{-2}, M = average molar mass of nickel and cobalt is 58·8 g mol^{-1} and ϕ is the electrodeposition efficiency, (m/tA) is also the mass electrodeposition rate.

From table 2, it can be seen that electrodeposition of Ni–Co alloys have higher current efficiencies in the presence of a magnetic field compared to the behaviour without a magnetic field for every concentration of cobalt in nickel Watts bath. The hydrogen evolution reaction (HER) was increased with PPMF but the increasing of HER is not much as the increasing of metals on the electrode surface. In mildly acidic solution, the HER can arise from these reactions at the cathode:

$$2H^+ (aq) + 2e^- \rightarrow H_2 (g),$$

$$2H_2O (l) + 2e^- \rightarrow H_2 (g) + 2OH^- (aq).$$

Electrodeposition of Ni–Co is much enhanced compared to the HER because some of the HER comes from the water molecules which does not carry charges, so the water molecules does not experience Lorentz force and Paramagnetic force with the presence of a magnetic field. The proton carries a single positive charge which experiences a smaller Lorentz force compared to the Lorentz force experienced by the nickel and cobalt ions which both are double charged ions. The paramagnetic force which is much larger for the nickel and cobalt ions makes the electrodeposition of Ni–Co alloys have higher current efficiencies with the presence of magnetic field compared to the HER.

3.2 *SEM and EDX analysis and characterization of Ni–Co alloys*

Deposited Ni–Co alloys were also investigated using SEM and EDX. From EDX analysis, it was discovered that the electrodeposition of cobalt was enhanced compared to nickel despite concentration of Co is lower than the amount of nickel in Watt's bath (0 to 5%). Magnetic moment of cobalt is greater than nickel[11], thus larger magnetic susceptibility can be observed for Co^{2+} than Ni^{2+}. The increased paramagnetic force and field gradient force of the Co^{2+} ions will thus enhance the cobalt electrodeposition. The figure 3 shows that the electrodeposition of Cobalt was enhanced with the presence of a PPMF. Some authors have also agreed that Paramagnetic Force has a larger effect on electrodeposition compared to Lorentz Force.[22,23] Hinds *et al*[9] have estimated that Paramagnetic Force have a force density of 10^4 Nm^{-3} compared to Lorentz Force of only 10^3 Nm^{-3}.

Figures 4a and b show the SEM image of Ni–Co surfaces which was electrodeposited at 75 mA cm^{-2} using Ni Watt's solution in alkaline medium with the absence and presence of a magnetic field respectively. At this stage, it cannot be determined exactly the effect of an applied magnetic field towards the crystallite sizes of the Ni–Co alloy from the SEM micrograph alone. But other workers[18,25–27] have reported that an applied magnetic field gave larger crystallite size for cobalt electrodeposition because of an increased mass transport. They also reported that holes on the surface of the cobalt deposit from the effect of hydrogen evolution reaction had disappeared with the application of a magnetic field.[14,16–18] An increased mass transport of cobalt ions have diminished the effect of hydrogen evolution reaction under magnetic field which gave larger cobalt crystallites, prevented the appearance of holes attributed to hydrogen evolution reaction and gave more dense cobalt deposits.

3.3 *X-Ray diffraction (XRD) studies*

The Ni–Co fabricated film characterized via the X-ray diffraction (XRD). Ibro *et al*[18] have attempted to

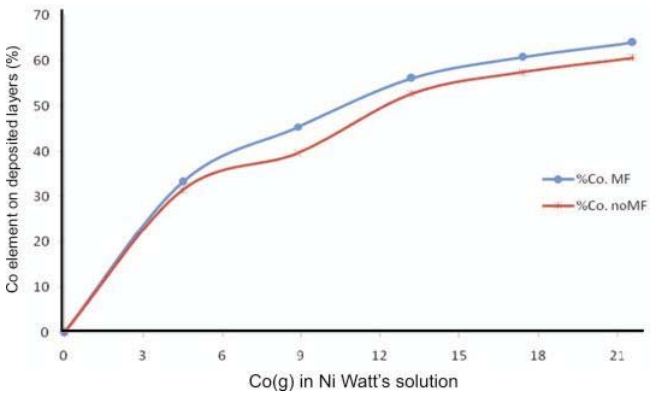

Figure 3. The %mass deposition rate of Co compare to Ni at the presence and absence of MF (4.4T) via different doses of Co in the nickel Watt's solution.

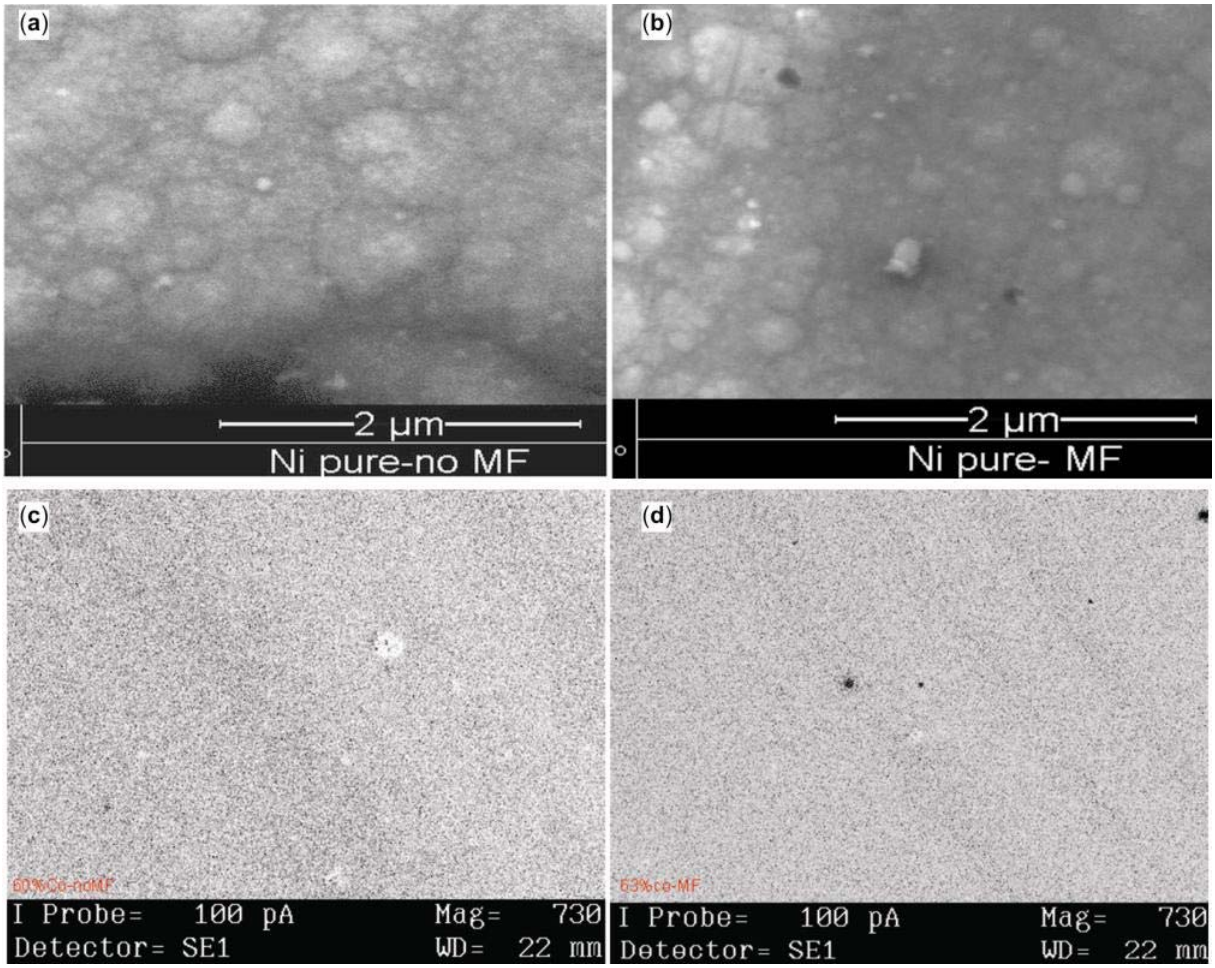

Figure 4. SEM micrographs of Ni and Ni–Co deposits obtained at 75 mA cm^{-2} for 7 min Nickel Watt's bath based on copper plate; (**a**) Ni in the absence of MF; (**b**) Ni in the presence of a MF at 4·4T; (**c**, **d**) Ni–Co deposited in same bath solution which; (**c**) Ni–Co in the absence of MF; (**d**) in the presence of PPMF 4·4T.

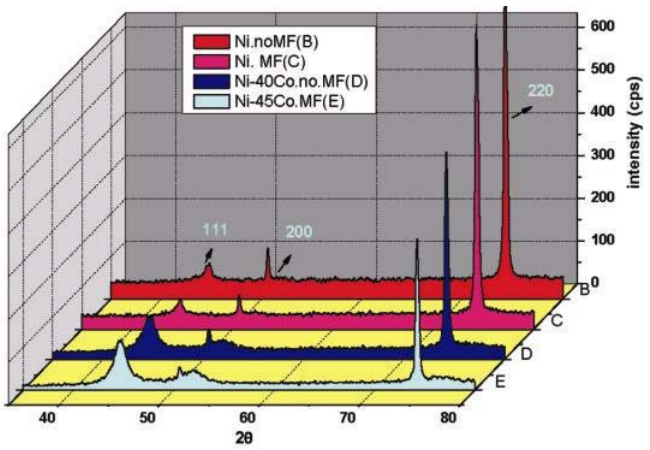

Figure 5. XRD spectra of Ni–Co layers with and without PPMF (4·4 T) at different amount of cobalt.

prove the texture and morphology of electrodeposited layers could be changed with the applied external magnetic field. The growth of fine grains with texture (200) were enhanced with PPMF as it was shown on figure 5. The XRD figure has illustrated at the presence of Tiourea the full width at half maximum (FWHM) of textures (200) were broadened with increasing of cobalt and applied PPMF as well. The intensity of peaks (220) was shrunk with increasing of cobalt and Magnetic flux. To controversy, the intensity of textures (200, 111) was enlarged with the enhancing of cobalt on the electrodeposited Ni–Co alloy films. The grain size changing of deposited layers could be calculated from XRD data through the Debye–Scherrer equation[27]

$$l = \frac{0{\cdot}9\lambda}{FWHM\cos\theta_c},$$

where $\lambda = 1{\cdot}540$ Å is the wavelength, full width at half maximum (in radians), l is the grain size/nm

Table 3. The polarization resistance was increased with increasing of cobalt in Ni–Co alloys. Furthermore, at the same concentration solution (Ni Watt's + 8·9 Co gl^{-1}) the Ni–Co alloy was deposited with higher percentage of cobalt due to the influence of PPMF, hence the polarization resistance was increased.

Ni-Co Alloy	Polarization resistance, R_p/ohm cm^{-2}
25% Co deposited with PPMF [Ni Watt's + 4·5Co (g/l)]	$6{\cdot}33 \times 10^{+5}$
40% Co deposited without PPMF [Ni Watt's + 8·9Co (g/l)]	$6{\cdot}50 \times 10^{+5}$
45% Co deposited with PPMF [Ni Watt's + 8·9Co (g/l)]	$7{\cdot}28 \times 10^{+5}$
60% Co deposited with PPMF [Ni Watt's + 17·4Co (g/l)]	$8{\cdot}15 \times 10^{+5}$

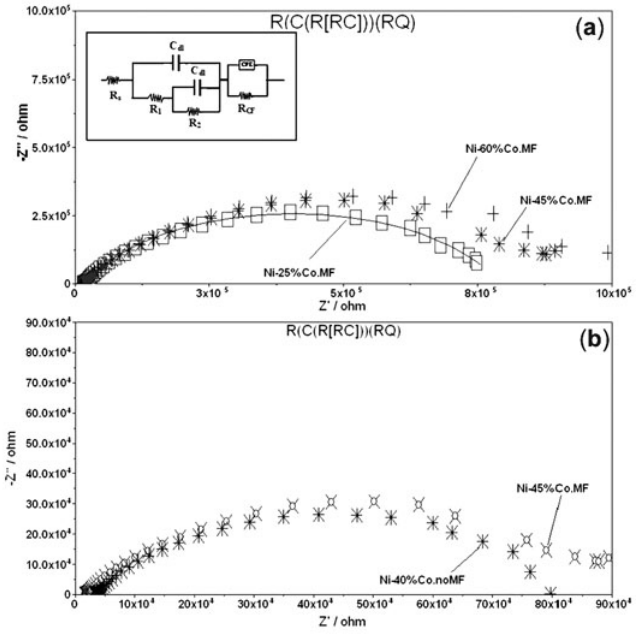

Figure 6. AC corrosion analysis method (Nyquist plot); through the polarization resistance (R_p) via magnitude of semi circle diameter; (**a**) the increasing R_p with increasing Co content in Ni–Co Alloy; (**b**) the increasing of semi circle diameter through presence of PPMF (4·4T) compare with the absence of PPMF for Ni–Co alloy deposited in same concentration of electrodeposition bath.

and θ_c is the angle satisfying Bragg's law. However, the determination of grain size and strain for alloy compounds are complex via data of XRD.[27] It is depended to fraction on compounds in alloys. The texture and morphological changes of Ni–Co deposited layers were carried out due to the influence of PPMF to the electrode surface induced a convective solution flow in electrode's vicinity, decreasing the thickness of Nernest layer. Koza *et al*[28] has shown the size of hydrogen bubble crucially reduced with PPMF hence the area could be enlarged for nucleation of metals on the electrode surface.

3.4 *Corrosion measurements*

Dissolution of Ni–Co deposited alloys was investigated in 3·5% seawater salinity.[12] The general trend of the impedance measurements is in agreement with expectation, as the Polarization resistance (R_p) is smaller for lower Co content in Ni–Co alloys deposited with a presence of PPMF as shown in figure 6a and larger R_p values for Ni–Co alloys deposited with a presence of PPMF than without a PPMF as shown in figure 6b. Table 3 presents the polarization resistance R_p values for different Ni–Co alloys.

From the Nyquist plots, the best fitting (figure 6) was carried out when double layer capacitance was replaced with constance phase element (CPE). These results indicated that the substrate surface was not smooth.The double layer capacitance can be represented by a CPE, where,

$$Z(CPE) = \frac{1}{T(jw)n},$$

where n is a number between 0 and 1. The CPE n value from the FRA software were found to be in ranges of 0·71–0·75, which is in agreement for a rough surface area.[29]

4. Conclusion

The influence of various concentration of Co on electrodeposition of Ni–Co alloys was studied in the absence and presence of PPMF ($\Delta m = 0{\cdot}07$ to $0{\cdot}12$ mg cm^{-2} min^{-1}). PPMF has increased the rate of metal electrodeposition. Both Ni^{2+} and Co^{2+} are doubly charged ions and will experience Lorentz force in solution in the presence of a PPMF, hence causing convection which increases mass transport and the rate of electrodeposition. With the presence of PPMF, cobalt electrodeposition rate was clearly

enhanced compared to nickel in the Ni–Co alloys (0 to 5%), due to larger magnetic moment for cobalt, which an increase in the field gradient force and paramagnetic force for the Co^{2+} ions in solution. Corrosion measurements showed that the electrodeposits of the Ni–Co alloys in the presence of a PPMF have larger polarization resistance R_p, than without the PPMF, and the increase in the Co content in the Ni–Co alloys gave larger polarization resistance. Increased current efficiencies were also seen for electrodeposition of Ni–Co alloys with the presence of a magnetic field compared to without a magnetic field.

Acknowledgements

We would like to thank the University of Malaya for financial support from University Research Grant PS 388/2008C, UMCiL grant (TA009/2008A) and (TA007/2009A). One of the authors (M Ebadi) acknowledges University of Malaya for Fellowship.

References

1. Bagotzky, V S 1993 *Fundamentals of electrochemistry* (New York: Plenum Press) p. 404
2. *Metal Finishing Guidebook and Dictionary* (New York, USA: Elsevier Science Publication), Published Annually
3. Brenner A 1963 *Electrodeposition of alloys. Principles and practice* (New York and London: Academic Press) vols 1 and 2
4. Hessami, S and Tobias C W 1989 *J. Electrochem. Soc.* **136** 3611
5. Georgiev G S, Georgieva V T and Plieth W 2005 *Electrochim. Acta* **51** 870
6. Fahidy T Z 2001 *Prog. Surf. Sci*. **68** 155
7. Krause A, Uhlemann M, Gebert A and Schultz L 2004 *Electrochim. Acta* **49** 4127
8. Shannon J C, Gu Z H and Fahidy T Z 1997 *J. Electrochem. Soc*. **144** L314
9. Tacken, R A and Janssen L J J 1995 *J. Appl. Electrochem*, **25** 1
10. Hinds G, Coey J M D and Lyons M E G 2001 *Electrochem. Comm*. **3** 215
11. Carlin R L 1986 *Magnetochemistry* (Springer-Verlag)
12. Jons D A 1996 *Principles and prevention of corrosion* (Prentice Hall)
13. Walsh F C 1992 *Trans. Inst. Metal Finish* **70** 50
14. Krause A, Hamann C, Uhlemann M, Gebert A and Schultz L 2005 *J. Magnetism and Magnetic Mater.* **290–291** 261
15. Uhlemann M, Krause A and Gebert A 2005 *J. Electroanal. Chem*. **577** 19
16. Matsushima H, Ispas A, Bund A, Plieth W and Fukunaka Y 2007 *J. Solid State Electrochem.* **11** 737
17. Krause A, Koza J, Ispas A, Uhlemann M, Gebert A and Bund A 2007 *Electrochim. Acta* **52** 6338
18. Tabakovic I, Riemer S, Vas'ko V, Sapozhnikov V and Kief M 2003 *J. Electrochem. Soc.* **150** C635
19. Msellak K, Chopart J P, Jbara O, Aaboubi O and Amblard J 2004 *J. Magnetism and Magnetic Mater* **281** 295
20. Ebadi M, Basirun W J and Alias Y 2009 *Asia J. Chem.* **21(9)** 7354
21. Ispas A, Matsushima H, Plieth W and Bund A 2007 *Electrochim. Acta* **52** 2785
22. Mori S, Satoh K and Tanimoto A 1994 *Electrochim, Acta*. **39** 2789
23. Mori S, Kumita M, Takeuchi M and Tanimoto A 1996 *J. Chem. Eng. Jpn* **29** 229
24. Gu Z H and Fahiday T Z 1987 *J. Electrochem. Soc.* **134** 2241
25. O'Brien R N and Santhanam K S V 1997 *J. Appl. Electrochem*. **27** 573
26. Waskaas M and Kharkats Y I 1999 *J. Phys. Chem.* **B103** 4876
27. Ganesh, V, Vijayaraghavan D and Lakshminarayanan V 2005 *Appl. Sur. Sci*. **240** 286
28. Koza J A, Muhlenhoff S, Uhlemann M and Eckert K 2009 *Electrochem. Com.* **11** 425
29. Barsukov E and MacDonald J R (eds) 2005 *Impedance spectroscopy* (John Wiley and Sons) 2nd edn, pp 494–495